Biochemical and Biophysical Research Communications 460 (2015) 983–988

Contents lists available at ScienceDirect

Biochemical and Biophysical Research Communications

journal homepage: www.elsevier.com/locate/ybbrc

Fenofibrate suppressed proliferation and migration of human neuroblastoma cells via oxidative stress dependent of TXNIP upregulation

Cunjin Su [a, 1], Aiming Shi [a, 1], Guowen Cao [a], Tao Tao [c], Ruidong Chen [b], Zhanhong Hu [a], Zhu Shen [a], Hong Tao [a], Bin Cao [a], Duanmin Hu [b, *], Junjie Bao [a, *]

[a] Department of Pharmacy, The Second Affiliated Hospital of Soochow University, Suzhou, 215004, People's Republic of China
[b] Department of Gastroenterology, The Second Affiliated Hospital of Soochow University, Suzhou, 215004, People's Republic of China
[c] Department of Urology, Zhongda Hospital, Medical School of Southeast University, Nanjing, 210009, People's Republic of China

ARTICLE INFO

Article history:
Received 20 March 2015
Available online 1 April 2015

Keywords:
Fenofibrate
TXNIP
Neuroblastoma
Oxidative stress
Apoptosis
SHSY5Y

ABSTRACT

There are no appropriate drugs for metastatic neuroblastoma (NB), which is the most common extra-cranial solid tumor for childhood. Thioredoxin binding protein (TXNIP), the endogenous inhibitor of ROS elimination, has been identified as a tumor suppressor in various solid tumors. It reported that fenofibrate exerts anti-tumor effects in several human cancer cell lines. However, its detail mechanisms remain unclear. The present study assessed the effects of fenofibrate on NB cells and investigated TXNIP role in its anti-tumor mechanisms. We used MTT assay to detect cells proliferation, starch wound test to investigate cells migration, H_2DCF-DA to detect intracellular ROS, siRNA to interfere TXNIP and peroxisome proliferator-androgen receptor-alpha (PPAR-α) expression, western blot to determine protein levels, flow cytometry to analyze apoptosis. Fenofibrate suppressed proliferation and migration of NB cells, remarkably increased intracellular ROS, upregulated TXNIP expression, promoted cell apoptosis. Furthermore, inhibition of TXNIP expression attenuated anti-tumor effects of fenofibrate, while inhibition of PPAR-α had no influences. Our results indicated the anti-tumor role of fenofibrate on NB cells by exacerbating oxidative stress and inducing apoptosis was dependent on the upregulation of TXNIP.

1. Introduction

Neuroblastoma (NB) is one of the most frequent extra-cranial solid tumors in children arising from neural crest sympathoadrenal progenitor cells [1]. NB therapy advances have led to notably improved outcomes for children. However, approximately 50% of children with NB is a clinical aggressive form, and the overall survival rates are less than 40% [2]. It lacks effective treatment for high-risk NB, which accounts for 12% of paediatric cancer deaths [3]. Therefore, we need to find novel effective agents for NB therapy.

Fenofibrate, a specific agonist of PPAR-α, belongs to the nuclear-hormone-receptor family. Fenofibrate has been used to treat different forms of hyperlipidemia and hypercholesterolemia [4]. Interestingly, recent studies show that fenofibrate may have anti-tumor effects by directly attenuating tumor growth. Although it reported fenofibrate had anti-tumor effects in glioma, lung cancer, prostate cancer, hepatocelluar carcinoma [5–9], its effect on NB has rarely been reported. Researchers found fenofibrate resulted in G1 phase arrest [10], attenuated gap junctional coupling between cancer cells [11], but the detail mechanisms of fenofibrate anti-tumor effects are still unclear. However, many researchers reported fenofibrate increased intracellular ROS, and aggravated oxidative injury [5]. These findings indicate one or some protein importantly regulating oxidative stress may participate the anti-tumor role of fenofibrate.

Thioredoxin-interacting protein (TXNIP), also known as thioredoxin-binding protein-2 (TBP-2) or VD3 upregulated protein 1 (VDUP1), is an important negative regulator of thioredoxin (Trx) system, which is composed of thioredoxin, thioredoxin reductase, and NADPH [12]. TXNIP is the endogenous inhibitor of reactive oxygen species (ROS) elimination, by binding to the active cysteine

* Corresponding authors. The Second Affiliated Hospital of Soochow University, San Xiang Road No.1055, Suzhou, 215004, Jiangsu Province, People's Republic of China. Fax: +86 512 67783686.
E-mail addresses: hudmsdfey@sina.com (D. Hu), baojjsdfey@sina.com (J. Bao).
[1] These authors contributed equally to this work.

http://dx.doi.org/10.1016/j.bbrc.2015.03.138
0006-291X/

residue of Trx, resulting in oxidative stress [13]. TXNIP mediates inhibition of cell proliferation and pro-apoptotic function via activation of apoptosis signal regulating kinase1 (ASK1) [14]. TXNIP expression is suppressed in a series of tumor cells, including gastric, breast and bladder cancers [15,16]. Growing evidences suggest TXNIP could be a tumor suppressor [17,18], but its role in NB has not been reported. The present study aims to explore the effects of fenofibrate on the proliferation and migration of NB cells, and to investigate TXNIP roles in oxidative injury induced by fenofibrate in NB cells.

2. Materials and methods

2.1. Reagents and antibodies

Fenofibrate and H_2DCF-DA were purchased from Sigma Chemicals. DMEM/F12 and fetal bovine serum (FBS) were purchased from Hyclone. siRNAs were synthesized by GenePharma (Shanghai, China). TXNIP, PPAR-α, GAPDH antibodies were purchased from Signalway Antibody. Goat anti-rabbit and rabbit anti-goat IgG horseradish peroxidase (HRP)-conjugated secondary antibodies, trypsin, MTT kit and crystal violet were purchased from Beyotime Biotechnology. Polyvinylidene difluoride (PVDF) membrane was purchased from Millipore. Apoptosis detection kit was purchased from BD (Material Number: 559763). Lip2000 transfection reagent was purchased from Invitrogen.

2.2. Cell culture

Neuroblastoma cell lines including SHSY5Y and IMR-32 were purchased from Shanghai Cell Bank, Chinese Academy of Sciences. SHSY5Y and IMR-32 cells were cultured in DMEM/F12 medium supplemented with 10% FBS. Cells were cultured as a monolayer in 5% CO_2 in a humidified incubator at 37 °C.

2.3. Assay of MTT conversion

Cells were seeded into 96-well plates (Cyagen) at a density of 10^4 cells/well in 200 μl culture medium. After treatment, the medium was replaced with 200 μl DMEM/F12 contained 0.5 mg/ml MTT and incubated at 37 °C for 4 h. Afterwards, the supernatant was sucked out, and cells were lysed in 200 μl DMSO for 10 min at 37 °C. The optical density (OD) values were measured at 490 nm using a plate reader. The obtained values were presented as folds of the control group respectively.

2.4. Detection of intracellular ROS

H_2DCF-DA was used to detect intracellular generation of ROS following the reference [19]. After treatment, SHSY5Y cells were incubated with 25 μM H_2DCF-DA for 30 min. After washed 3 times with cold PBS, cell images were acquired immediately by fluorescence microscopy. Intracellular ROS intensity was measured by Imagepro Plus software.

2.5. Western blot analysis

Cells were washed with ice PBS for 3 times and lysed with RIPA lysate containing PMSF on ice for 45 min. Samples were centrifuged for 15 min at 12,000 rpm at 4 °C and the supernatants were collected. Protein (60 μg for each extract) was resolved by 10% SDS-PAGE, electroblotted to PVDF membrane, and blocked in 5% non-fat milk at room temperature. Membranes were incubated with primary antibodies overnight at 4 °C. Membranes were washed by TBST and probed with HRP-conjugated anti-rabbit or anti-goat IgG respectively.

2.6. siRNA transfection

SHSY5Y cells were cultured in 96-well plates (1×10^4 cells/well) or in 6-well plates (5×10^5 cells/well). To inhibit TXNIP and PPAR-α expression, TXNIP siRNA (5′-CAU CCU UCG AGU UGA AUA UTT-3′), PPAR-α siRNA (5′-UCA CGG AGC UCA CAG AAU UUU-3′) or negative control siRNA was transfected using Lip2000 transfection reagent in accordance with the manufacture's protocol (5 pmol for 96-well plate, 120 pmol for 6-well plate). The cells were transfected with siRNAs for 48 h.

2.7. Scratch wound assay

Cells seeded in 6-well plates (5×10^5 cells/well) were scratched with a sterile plastic 10 μl micropipette tip. Cells were washed 3 times with ice PBS to remove loose and detached cells. Cell images were acquired immediately and 48 h after the scrape.

2.8. Colony formation assay

In total, 2×10^3 SHSY5Y cells/well were placed into 6-well plate. After incubation of 100 μM fenofibrate for 10 days, visible colonies were fixed with 4% methanol for 30 min and then stained with 0.1% crystal violet for 20 min. The plates were washed by water for 3 times, and dried for 1 h at 37 °C. Crystal violet absorbed in cells was dissolved in 10% acetic acid. OD values were measured at 595 nm. The obtained values were presented as folds of control.

2.9. Apoptosis assay

SHSY5Y cells were seeded in 6-well plates for 24 h and then were treated with 100 μM fenofibrate for 48 h. Subsequently, the cells were collected by trypsinization, and washed twice with cold PBS, then resuspend in binding buffer. Added 5 μl of Annexin V and 5 μl 7-AAD in 100 μl suspension, incubated at room temperature for 15 min in the dark. Finally, added 400 μl binding buffer, and analyzed by flow cytometry.

2.10. Statistical analysis

Data were presented as mean ± SD. Statistical comparisons were analyzed by one-way ANOVA and Student's test using the SPSS 13.0 software. $p < 0.05$ was considered as statistically significant.

3. Results

3.1. Fenofibrate inhibited neuroblastoma cells proliferation

Two human neuroblastoma cells, SH-SY5Y and IMR-32, were treated with fenofibrate at different concentrations (0, 12.5, 25, 50, 100 and 200 μM, DMSO in each group was balanced) for 48 h to verify the anti-tumor effects of fenofibrate. To investigate the cytostatic effects of fenofibrate, MTT assay was used to determine cell growth rate. The results showed that fenofibrate inhibited the proliferation of SHSY5Y and IMR-32 in a dose-dependent manner. More than 50% cell growth inhibition was observed at 100 μM fenofibrate both in SHSY5Y and IMR-32 cells compared with the DMSO-treated control respectively (Fig. 1A and B, $p < 0.001$). It was notable that 100 μM fenofibrate was the most profound concentration to inhibit cell proliferation both in SHSY5Y and IMR-32 cells. DMSO alone had no effect on cells viability. Hoechst staining showed 100 μM fenofibrate significantly induced SHSY5Y and IMR-

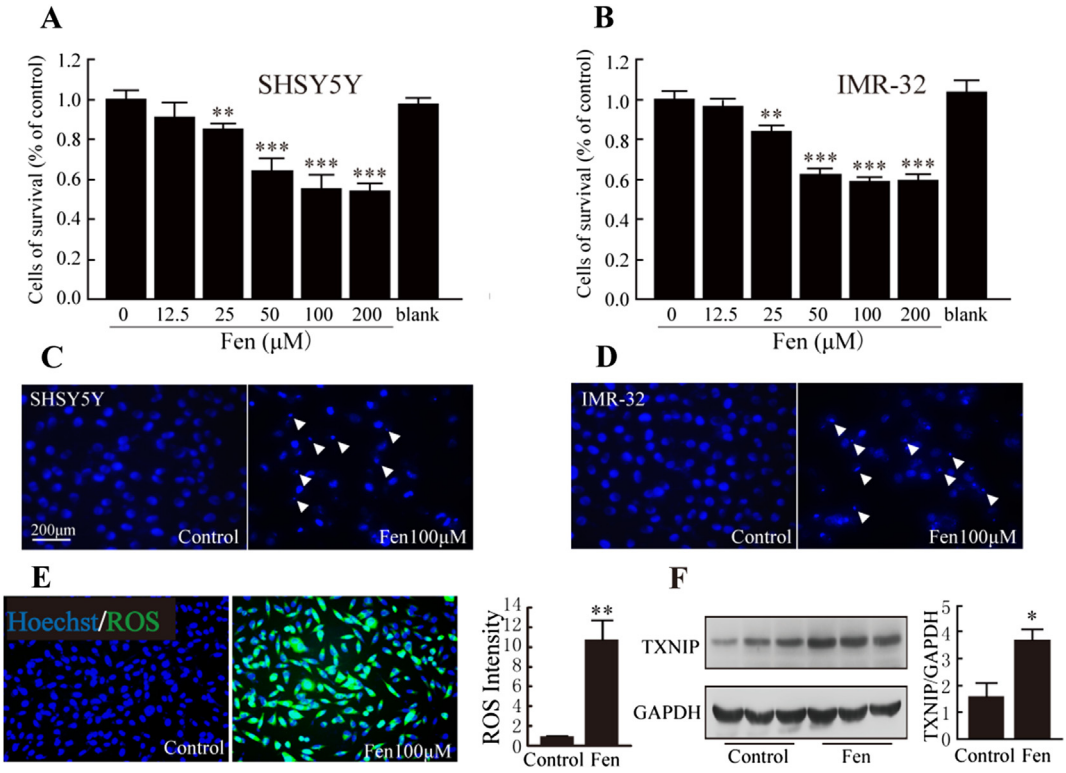

Fig. 1. Fenofibrate inhibited viability of NB cells, increased intracellular ROS and induced TXNIP expression. (A, B) SHSY5Y and IMR-32 cells viability was measured by MTT assay following treatment of different concentrations of fenofibrate for 48 h. Blank group was not treated with fenofibrate or DMSO. (C, D) Nuclear of SHSY5Y and IMR-32 cells was stained by Hoechst. (E) Intracellular ROS of SHSY5Y cells was detected by H_2DCF-DA (green fluorescence), and ROS intensity was analyzed by Imagepro Plus. (F) TXNIP was determined by western blot, GAPDH was detected as a loading control. $^{*}p < 0.05$, $^{**}p < 0.01$, $^{***}p < 0.001$ vs. control group. n = 3. Fen represents fenofibrate. (For interpretation of the references to color in this figure caption, the reader is referred to the web version of this article.)

32 cells karyopyknosis (Fig. 1C and D). So, cells were treated with 100 μM fenofibrate for 48 h in the following experiments.

3.2. Fenofibrate increased intracellular ROS and induced TXNIP expression

After fenofibrate treatment, intracellular ROS was detected by H_2DCF-DA. As show in Fig. 1E, incubation with 100 μM fenofibrate in SHSY5Y cells for 48 h resulted in a significant accumulation of intracellular ROS. It showed that the intensity of ROS fluorescence increased 10-fold in SHSY5Y cells following the fenofibrate incubation (Fig. 1E, $p < 0.01$). Growing evidences now point that TXNIP is an importantly endogenous inhibitor of ROS elimination and plays anti-tumor roles in several tumor cells. We found TXNIP expression increased to an almost 2-fold compared with control group after 48 h incubation with 100 μM fenofibrate in SHSY5Y cells (Fig. 1F, $p < 0.05$). These results indicated that fenofibrate induced ROS accumulation via the upregulation of TXNIP.

3.3. Anti-proliferation and anti-migration effects of fenofibrate depended on TXNIP upregulation

Fenofibrate induced TXNIP expression, so whether TXNIP participated the anti-tumor role of fenofibrate? In addition, as an agonist of PPAR-α, the question whether PPAR-α mediated anti-tumor role of fenofibrate on NB cells should be answered. Therefore, we used TXNIP and PPAR-α siRNAs to interfere the protein expression. As show in Fig. 2A and B, TXNIP was decreased 70%, and PPAR-α was decreased 55% by respective siRNA (treated for 48 h) compared with the control group respectively. Furthermore, we explored the cell death induced by fenofibrate after TXNIP and PPAR-α depletion. Interestingly, depletion of TXNIP attenuated the anti-proliferation effect of fenofibrate (Fig. 2C and D, $p < 0.001$). However, depletion of PPAR-α had no influence on fenofibrate-induced cytotoxicity in SHSY5Y cells (Fig. 2C). Fenofibrate treatment also resulted in complete inhibition of SHSY5Y clonogenic growth (Fig. 2E), which further supported its anti-proliferative effect. Wound scratch assay was used to evaluate effect of fenofibrate on SHSY5Y cells migration. Scratch baseline width was 748 μm. After 48 h, the width was 306 μm in control well, and it was 555 μm in fenofibrate-treated well. But scratch width was 344 μm in TXNIP siRNA pretreatment well, and was significantly narrower than fenofibrate-treated alone (Fig. 2F, $p < 0.01$). These results indicated that the anti-proliferation and anti-migration effects of fenofibrate in NB cells were dependent on the upregulation of TXNIP, while were independent on the activation of PPAR-α.

3.4. Apoptosis induced by fenofibrate depended on TXNIP upregulation

We detected apoptosis by flow cytometry. Apoptosis cells accounted for 36% in fenofibrate-treated group, the percent was 3-fold compared with control (Fig. 3A, $p < 0.01$). The percent of apoptosis cells was 13% in TXNIP siRNA-pretreated group, and was significantly lower compared with fenofibrate-treated cells (Fig. 3A, $p < 0.01$). Furthermore, given that apoptosis-promoting protein Bax and caspase3, and apoptosis-inhibiting protein Bcl-2 are key regulators of apoptosis, we investigated the influences of fenofibrate on these protein expressions. We found expression of apoptosis-inhibiting protein Bcl-2 was dramatically decreased to 50%

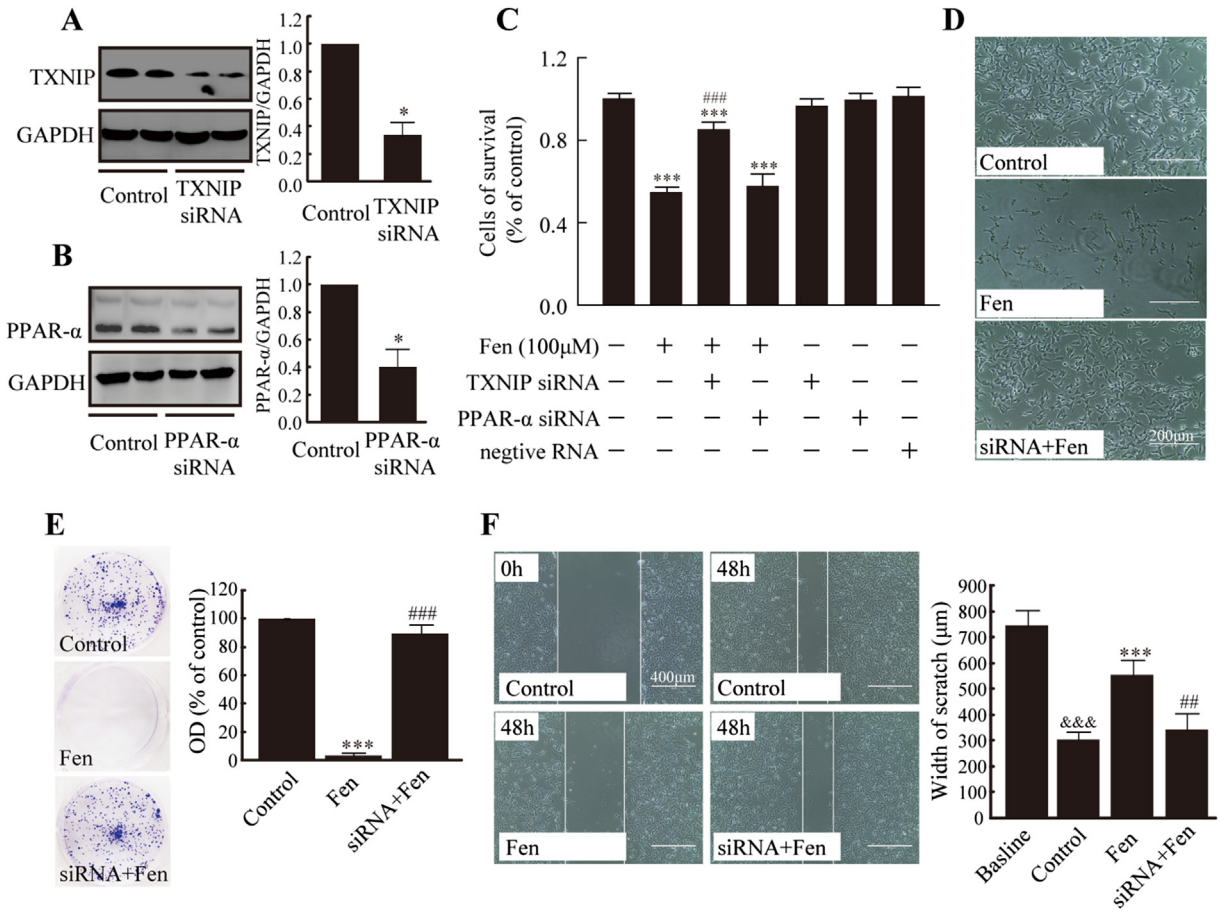

Fig. 2. TXNIP mediated anti-proliferation and anti-migration effects of fenofibrate in SHSY5Y cells. (A, B) TXNIP and PPAR-α were determined by western blot after transfection with siRNA respectively for 48 h. (C) Cell viability was measured by MTT assay. (D) Cell morphology was obtained by microscope in bright field. (E) Colony formation assay was performed in SHSY5Y cells after treatment with fenofibrate for 48 h. (F) Cells migration ability was estimated quantitatively by measuring the remaining width between the two edges of the wound. $^{*}p < 0.05$, $^{***}P < 0.001$ vs. control group; $^{\#\#}p < 0.01$, $^{\#\#\#}p < 0.001$ vs. fenofibrate-treated group; $^{\&\&\&}p < 0.001$ vs. baseline. n = 3. Fen represents fenofibrate, siRNA represents TXNIP siRNA in (D), (E) and (F).

compared with control cells (Fig. 3B, $p < 0.01$). On the other hand, Bax, related to apoptosis-promoting process, was increased to 2-fold vs. control cells (Fig. 3B, $p < 0.01$). Moreover, fenofibrate facilitated the activation of caspase3. Cleavage caspase3 was increased to 2-fold after fenofibrate treatment in SHSY5Y cells (Fig. 3B, $p < 0.05$). However, TXNIP siRNA attenuated or abolished fenofibrate influences on regulation of Bcl-2, Bax and caspase-3 activation (Fig. 3B, $p < 0.05$). In short, fenofibrate induced apoptosis of SHSY5Y cells via downregulation of Bcl-2 and upregulation of Bax, resulting in activation of caspase-3 finally. And these roles were dependent on TXNIP over-expression.

4. Discussion

Fenofibrate, a PPAR-α agonist commonly used in the treatment for hyperlipidemia and hypercholesterolemia, has been recognized to exert anti-proliferative and pro-apoptotic effects in several tumor cell lines [4,7,8,10]. But it rarely reported its roles of fenofibrate in NB. Our present study showed that fenofibrate suppressed NB cells (including SHSY5Y and IMR-32) proliferation and migration, upregulated TXNIP expression, triggered oxidative stress by remarkably increased intracellular ROS, inhibited cellular survival pathway mediated by AKT phosphorylation. Moreover, we demonstrated the anti-tumor effects of fenofibrate in NB cells were dependent on TXNIP by siRNA transfection. These findings indicated fenofibrate maybe a potential usefulness drug for NB therapy, and TXNIP played key roles in the process.

ROS plays key roles for cellular survival. Low and normal concentration ROS is benefit for cellular survival, while high concentration ROS is injurious for protein, lipid and DNA [20]. Cancer progression has been associated with oxidative stress [21], which is mainly mediated by ROS. Previous studies reported PPAR-α agonist can result in intracellular ROS accumulation [7]. In the present study, we found the intracellular ROS in SHSY5Y cells treated with fenofibrate was significantly increased. This suggested ROS played an important role in SHSY5Y cells apoptosis induced by fenofibrate.

TXNIP is a major regulator of cellular redox status by binding to and inhibiting thioredoxin, a principal protein acting as ROS scavenger [22]. So, TXNIP is a negative regulator of intracellular ROS. Furthermore, TXNIP inhibits cell invasion and metastasis, and promotes cell apoptosis [23]. It has shown that TXNIP is a tumor suppressor in cancer [17]. In present study, we found TXNIP was notably upregulated in SHSY5Y cells following fenofibrate treatment, suggesting TXNIP may mediate oxidative stress induced by fenofibrate. We speculated TXNIP was required for fenofibrate's anti-tumor role in NB cells. In addition, although fenofibrate is a PPAR-α agonist, several reports have demonstrated its anti-tumor effects are independent on PPAR-α activation [24]. To explore whether pro-apoptotic role of fenofibrate in NB cells were dependent on PPAR-α activation or TXNIP, we used siRNAs to interfere their expressions. Interestingly, our results suggested TXNIP, but

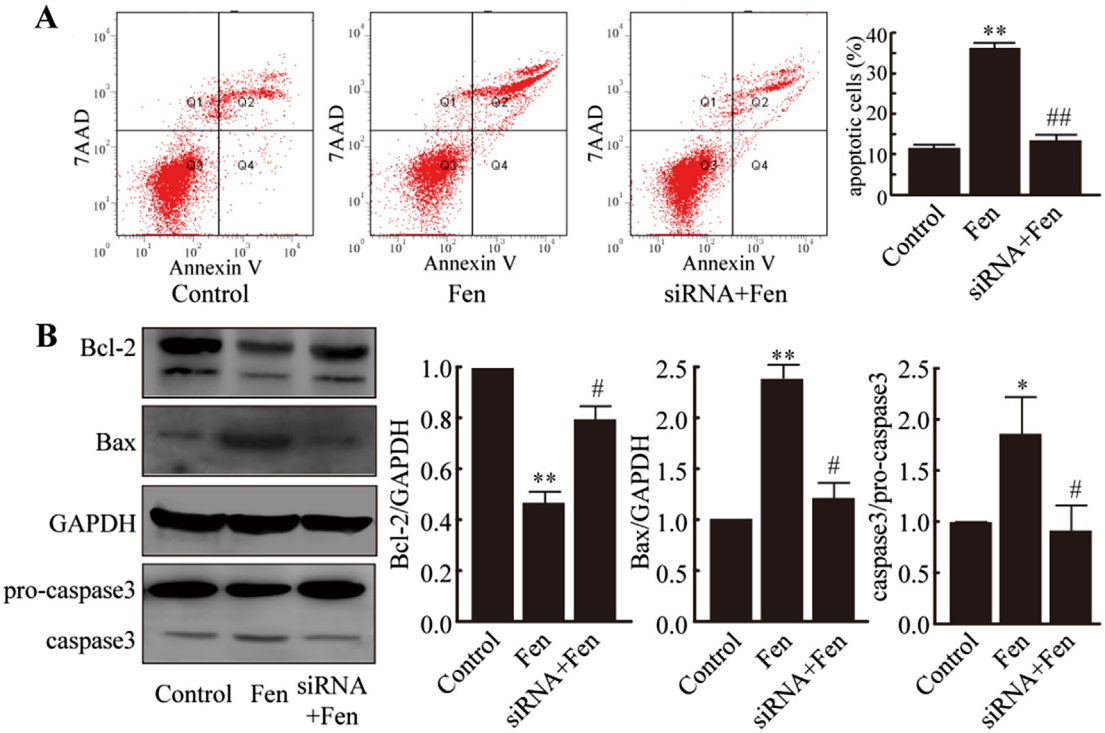

Fig. 3. TXNIP mediated the apoptosis induced by fenofibrate in SHSY5Y. (A) Apoptosis measured by flow cytometry analysis using Annexin V-FITC and 7-AAD staining following treatment with fenofibrate for 48 h. (B) Bcl-2, Bax and caspase3 were determined by western blot. $^{*}p < 0.05$, $^{**}p < 0.01$ vs. control group. $^{\#}p < 0.05$, $^{\#\#}p < 0.01$ vs. fenofibrate-treated group. n = 3. Fen represents fenofibrate, siRNA represents TXNIP siRNA.

not PPAR-α was required for the anti-tumor role of fenofibrate in NB cells. The results indicated TXNIP was not only a tumor suppressor, but also a target for anti-tumor drugs.

Capase3 plays a central role in the cascade reaction of apoptosis. Many apoptotic signalings, such as decrease of Bcl-2 and upregulation of Bax, would lead to activation of caspase3. Studies showed that fenofibrate decreased Bcl-2 expression, activated caspase-3, and resulted in apoptosis in mantle cell lymphoma and prostate cancer cells [24]. Consistent with the reports, our results showed fenofibrate significantly downregulated Bcl-2 expression, increased Bax expression and caspase3 cleavage. Interestingly, deletion of TXNIP by siRNA partly abrogated these roles of fenofibrate. It reported ROS resulted in apoptosis via downregulation of Bcl-2 [25]. Together, our results indicated TXNIP may be a upstream negative regulator of caspase3 via Bcl-2/Bax pathway, which was regulated by ROS.

In conclusion, our results indicated TXNIP was required for the anti-tumor role of fenofibrate in NB cells. However, it needs further research to explore the detail mechanisms of fenofibrate regulating TXNIP expression, and should verify its role in nude mice model.

Conflict of interest

We have no conflicts of interest to declare.

Acknowledgments

This work was supported partially by the Second Affiliated Hospital of Soochow University Science Foundation (NO. SDFEYQN1410 and NO. SDFEYBS1402), and Suzhou Science Foundation (NO. SYS201344).

References

[1] C. Bottino, A. Dondero, F. Bellora, L. Moretta, F. Locatelli, V. Pistoia, A. Moretta, R. Castriconi, Natural killer cells and neuroblastoma: tumor recognition, escape mechanisms, and possible novel immunotherapeutic approaches, Front. Immunol. 5 (2014) 56.

[2] T. Monclair, G.M. Brodeur, P.F. Ambros, H.J. Brisse, G. Cecchetto, K. Holmes, M. Kaneko, W.B. London, K.K. Matthay, J.G. Nuchtern, S.D. von, T. Simon, S.L. Cohn, A.D. Pearson, The International neuroblastoma risk group (INRG) staging system: an INRG task force report, J. Clin. Oncol. 27 (2009) 298–303.

[3] M.A. Smith, N.L. Seibel, S.F. Altekruse, L.A. Ries, D.L. Melbert, M. O'Leary, F.O. Smith, G.H. Reaman, Outcomes for children and adolescents with cancer: challenges for the twenty-first century, J. Clin. Oncol. 28 (2010) 2625–2634.

[4] M. Lella, K. Indira, A comparative study of efficacy of atorvastatin alone and its combination with fenofibrate on lipid profile in type 2 diabetes mellitus patients with hyperlipidemia, J. Adv. Pharm. Technol. Res. 4 (2013) 166–170.

[5] E. Binello, E. Mormone, L. Emdad, H. Kothari, I.M. Germano, Characterization of fenofibrate-mediated anti-proliferative pro-apoptotic effects on high-grade gliomas and anti-invasive effects on glioma stem cells, J. Neurooncol. 117 (2014) 225–234.

[6] H. Liang, P. Kowalczyk, J.J. Junco, S.H.L. Klug-De, G. Malik, S.J. Wei, T.J. Slaga, Differential effects on lung cancer cell proliferation by agonists of glucocorticoid and PPARalpha receptors, Mol. Carcinog. 53 (2014) 753–763.

[7] H. Zhao, C. Zhu, C. Qin, T. Tao, J. Li, G. Cheng, P. Li, Q. Cao, X. Meng, X. Ju, P. Shao, L. Hua, M. Gu, C. Yin, Fenofibrate down-regulates the expressions of androgen receptor (AR) and AR target genes and induces oxidative stress in the prostate cancer cell line LNCaP, Biochem. Biophys. Res. Commun. 432 (2013) 320–325.

[8] D. Yamasaki, N. Kawabe, H. Nakamura, K. Tachibana, K. Ishimoto, T. Tanaka, H. Aburatani, J. Sakai, T. Hamakubo, T. Kodama, T. Doi, Fenofibrate suppresses growth of the human hepatocellular carcinoma cell via PPARalpha-independent mechanisms, Eur. J. Cell. Biol. 90 (2011) 657–664.

[9] K.L. Zhang, L. Han, L.Y. Chen, Z.D. Shi, M. Yang, Y. Ren, L.C. Chen, J.X. Zhang, P.Y. Pu, C.S. Kang, Blockage of a miR-21/EGFR regulatory feedback loop augments anti-EGFR therapy in glioblastomas, Cancer Lett. 342 (2014) 139–149.

[10] D.F. Han, J.X. Zhang, W.J. Wei, T. Tao, Q. Hu, Y.Y. Wang, X.F. Wang, N. Liu, Y.P. You, Fenofibrate induces G/G phase arrest by modulating the PPARalpha/FoxO1/p27 pathway in human glioblastoma cells, Tumour Biol. (2015).

[11] E. Wybieralska, K. Szpak, A. Gorecki, P. Bonarek, K. Miekus, J. Drukala, M. Majka, K. Reiss, Z. Madeja, J. Czyz, Fenofibrate attenuates contact-stimulated cell motility and gap junctional coupling in DU-145 human prostate cancer cell populations, Oncol. Rep. 26 (2011) 447–453.

[12] P. Nguyen, R.T. Awwad, D.D. Smart, D.R. Spitz, D. Gius, Thioredoxin reductase as a novel molecular target for cancer therapy, Cancer Lett. 236 (2006) 164–174.
[13] E. Yoshihara, S. Masaki, Y. Matsuo, Z. Chen, H. Tian, J. Yodoi, Thioredoxin/Txnip: redoxisome, as a redox switch for the pathogenesis of diseases, Front. Immunol. 4 (2014) 514.
[14] K. Gao, Y. Chi, W. Sun, M. Takeda, J. Yao, 5′-AMP-activated protein kinase attenuates adriamycin-induced oxidative podocyte injury through thioredoxin-mediated suppression of the apoptosis signal-regulating kinase 1-P38 signaling pathway, Mol. Pharmacol. 85 (2014) 460–471.
[15] C.M. Woolston, S. Madhusudan, I.N. Soomro, D.N. Lobo, A.M. Reece-Smith, S.L. Parsons, S.G. Martin, Thioredoxin interacting protein and its association with clinical outcome in gastro-oesophageal adenocarcinoma, Redox Biol. 1 (2013) 285–291.
[16] C.M. Woolston, L. Zhang, S.J. Storr, A. Al-Attar, M. Shehata, I.O. Ellis, S.Y. Chan, S.G. Martin, The prognostic and predictive power of redox protein expression for anthracycline-based chemotherapy response in locally advanced breast cancer, Mod. Pathol. 25 (2012) 1106–1116.
[17] J.A. Morrison, L.A. Pike, S.B. Sams, V. Sharma, Q. Zhou, J.J. Severson, A.C. Tan, W.M. Wood, B.R. Haugen, Thioredoxin interacting protein (TXNIP) is a novel tumor suppressor in thyroid cancer, Mol. Cancer 13 (2014) 62.
[18] J. Zhou, Q. Yu, W.J. Chng, TXNIP (VDUP-1, TBP-2): a major redox regulator commonly suppressed in cancer by epigenetic mechanisms, Int. J. Biochem. Cell. Biol. 43 (2011) 1668–1673.
[19] X. Li, D. Zhen, X. Lu, H. Xu, Y. Shao, Q. Xue, Y. Hu, B. Liu, W. Sun, Enhanced cytotoxicity and activation of ROS-dependent c-Jun NH2-terminal kinase and caspase-3 by low doses of tetrandrine-loaded nanoparticles in Lovo cells–a possible trojan strategy against cancer, Eur. J. Pharm. Biopharm. 75 (2010) 334–340.
[20] S.W. Kang, S. Lee, E.K. Lee, ROS and energy metabolism in cancer cells: alliance for fast growth, Arch. Pharm. Res. (2015).
[21] B. Liu, W. Zhou, X. Chen, F. Xu, Y. Chen, J. Liu, Q. Zhang, S. Bao, N. Chen, M. Li, R. Zhu, Dihydromyricetin induces mouse hepatoma Hepal-6 cell apoptosis via the transforming growth factor-beta pathway, Mol. Med. Rep. 11 (2015) 1609–1614.
[22] R. Zhou, A. Tardivel, B. Thorens, I. Choi, J. Tschopp, Thioredoxin-interacting protein links oxidative stress to inflammasome activation, Nat. Immunol. 11 (2010) 136–140.
[23] F. Yamaguchi, Y. Hirata, H. Akram, K. Kamitori, Y. Dong, L. Sui, M. Tokuda, FOXO/TXNIP pathway is involved in the suppression of hepatocellular carcinoma growth by glutamate antagonist MK-801, BMC Cancer 13 (2013) 468.
[24] T. Li, Q. Zhang, J. Zhang, G. Yang, Z. Shao, J. Luo, M. Fan, C. Ni, Z. Wu, X. Hu, Fenofibrate induces apoptosis of triple-negative breast cancer cells via activation of NF-kappaB pathway, BMC Cancer 14 (2014) 96.
[25] S. Luanpitpong, P. Chanvorachote, C. Stehlik, W. Tse, P.S. Callery, L. Wang, Y. Rojanasakul, Regulation of apoptosis by Bcl-2 cysteine oxidation in human lung epithelial cells, Mol. Biol. Cell. 24 (2013) 858–869.